● 铝基复合材料　Aluminum Matrix Composites ●
DOI:10.16410/j.issn1000-8365.2023.3070

铝基复合材料激光粉末床熔化增材制造研究现状

朱昌隆[1],王洪泽[1,2],郭利萍[1],唐梓珏[1],母杰瑞[1],吴　一[1,2],黄　洁[3],胡凯明[3],王浩伟[1,2]
(1. 上海交通大学 材料科学与工程学院 金属基复合材料国家重点实验室,上海 200240; 2. 上海交通大学 安徽(淮北)陶铝新材料研究院,安徽 淮北 235000; 3. 上海飞机制造有限公司,上海 201324)

摘　要:采用激光粉末床熔化技术制备铝基复合材料在航空航天、军工、交通运输等领域显示出了深远的研究前景,向铝合金引入纳米增强体的种类、引入方式以及含量对铝合金可打印性、组织、力学性能产生的影响是学者们的关注热点。本文主要总结分析了 TiB_2、石墨烯、TiC 纳米增强体对激光粉末床熔化技术制备铝合金的晶粒形态、晶粒尺寸、相对密度、可打印性和力学性能的影响,进行了不同纳米增强体对打印态铝合金力学性能影响的对比,分析得出以 TiB_2 为代表的纳米增强体能够提升打印态铝合金的强度、塑性,使其具有良好的综合力学性能,最后提出了该研究领域在未来的进一步发展趋势。

关键词:增材制造;激光粉末床熔化;铝基复合材料;纳米增强体
中图分类号:TB333; TP391.73　　文献标识码:A　　文章编号:1000-8365(2023)07-0583-16

Research Status of Aluminum Matrix Composites Prepared by Laser Powder Bed Fusion Additive Manufacturing

ZHU Changlong[1], WANG Hongze[1,2], GUO Liping[1], TANG Zijue[1], MU Jierui[1], WU Yi[1,2], HUANG Jie[3], HU Kaiming[3], WANG Haowei[1,2]
(1. State Key Laboratory of Metal Matrix Composites, School of Materials Science & Engineering, Shanghai Jiao Tong University, Shanghai 200240, China; 2. Institute of Alumics Materials, Shanghai Jiao Tong University (Anhui), Huaibei 235000, China; 3. Shanghai Aircraft Manufacturing Co., Ltd., Shanghai 201324, China)

Abstract: Aluminum matrix composites prepared by laser powder bed fusion technology show profound research prospects in aerospace, military, transportation and other fields. The effects of the nano-reinforcement types, the methods of adding nano-reinforcements into aluminum alloys and the nano-reinforcement content on the printability, structure and mechanical properties of aluminum alloys are the main focus of researchers. This paper mainly summarized and analysed the effects of TiB_2, graphene and TiC nano-reinforcements on the grain morphology, grain size, relative density, printability, and mechanical properties of aluminum alloys prepared by laser powder bed fusion technology while providing a comparison of the effects of different nano-reinforcements on the mechanical properties of the as-built aluminum alloys. Analysis shows that the nano-reinforcements represented by TiB_2 can improve the strength and plasticity of the as-built aluminum alloys, resulting in a good comprehensive mechanical performance effect. Finally, this paper proposes further development trends for this research field in the future.

Key words: additive manufacturing; laser powder bed fusion; aluminum matrix composites; nano-reinforcements

收稿日期:2023-03-21
基金项目:国家自然科学基金(52075327,52004160);上海市青年科技英才扬帆计划(20YF1419200);上海市自然科学基金(20ZR1427500);淮北市重大科技项目(Z2020001);上海交通大学海外一流大学学术交流基金(2023 年度上海交通大学–康奈尔大学);国家商用飞机制造工程技术研究中心创新基金(3-0410300-031)
作者简介:朱昌隆,2000 年生,硕士研究生.研究方向为铝基复合材料激光增材制造. Email: 122050910046@sjtu.edu.cn
通讯作者:王洪泽,1989 年生,博士,副教授.研究方向为激光增材制造过程原位观测及高性能铝基复合材料研究. Email: hz.wang@sjtu.edu.cn
吴　一,1982 年生,博士,高级工程师.研究方向为激光增材制造高性能铝基复合材料研究. Email: eagle51@sjtu.edu.cn
引用格式:朱昌隆,王洪泽,郭利萍,等. 铝基复合材料激光粉末床熔化增材制造研究现状[J]. 铸造技术,2023,44(7): 583-598.
ZHU C L, WANG H Z, GUO L P, et al. Research status of aluminum matrix composites prepared by laser powder bed fusion additive manufacturing[J]. Foundry Technology, 2023, 44(7): 583-598.

铝及铝合金是具有轻质、良好延展性和抗腐蚀性等优点的金属[1-2]。激光粉末床熔化(laser powder bed fusion, LPBF)是金属材料增材制造的一种主要技术[3-6],具有近净成形、生产效率高、节省材料等优势[7-10]。近年来采用激光粉末床熔化技术制备铝及铝合金逐渐成为学者们关注的热点，然而材料的自身特性限制了该技术的进一步发展。一方面,在通常使用的波长为 1 064 nm 或 1 070 nm 的激光下[11],铝合金激光吸收率非常低(10%);另一方面,铝的高热导率(237 W/(m·K))[12]会加快打印过程中加热和冷却的速度。因此,如何避免铝及铝合金的激光粉末床熔化打印态样品普遍的粗大柱状晶组织,并进一步减少热裂纹缺陷的产生是亟待解决的难点[13-18]。

铝基复合材料(aluminum matrix composites, AMC)是解决铝及铝合金激光粉末床熔化打印难点的思路和方案。复合材料由两个或两个以上物理和化学性质不同的部分组成,包括连续的基体和不连续的增强相[19-20]。通过向铝合金引入 TiB_2、石墨烯、TiC 等纳米增强体[21-24],能够显著细化打印态样品的晶粒,改善铝合金在打印过程中的热裂纹问题[25-29]。并且铝基复合材料综合了铝、铝合金的优点以及纳米增强体高强度、高弹性模量的特点[30-32],具有优异的比强度、比刚度、耐磨性和低热膨胀系数,在航空航天、军工、交通运输等领域得到了广泛应用[33-36]。

本文总结分析了 TiB_2、石墨烯、TiC 纳米增强体对铝合金打印态样品的晶粒形态、晶粒尺寸、相对密度、可打印性和力学性能的影响,对比了现有主流的纳米增强体类型对打印态铝合金力学性能的影响,并提出了该研究领域未来的发展趋势。

1 TiB_2 增强

TiB_2 具有高熔点、高硬度、良好润湿性、与铝基体共格性良好等优点[35,37]。TiB_2 纳米颗粒的引入方式主要包含两大类:原位自生和外加法(球磨法、机械搅拌法等)[38-39]。在研究之初，铸造是用于制备 TiB_2 纳米颗粒增强铝基复合材料的主流方法之一，包括搅拌铸造、挤压铸造等[40-42],也有学者对其进行过半固态成形的研究[43]。近年来由于增材制造技术的迅速发展,对 TiB_2 纳米颗粒增强铝基复合材料激光粉末床熔化加工的研究不断增多。引入 TiB_2 纳米颗粒能够改变铝合金打印态样品的晶粒形态和尺寸,起到改善铝合金打印态样品相对密度、可打印性、力学性能等作用。

在铝合金打印态样品晶粒形态和尺寸的改变方面,上海交通大学 Guo 等[44]采用原位自生和气雾化法制备了 6%TiB_2/AlSi10Mg(质量分数)复合粉末,使用 AlSi10Mg 粉末作为对照材料，分别对两种粉末进行了激光粉末床熔化单轨扫描试验。借助 EBSD表征手段,发现 TiB_2 纳米颗粒的引入会导致柱状晶含量减少而等轴晶含量增多,起到了细化晶粒的作用。上海交通大学 Ding 等[45]通过原位自生制备了 2%TiB_2/Al-1.75%Fe-1.25%Ni(质量分数)复合粉末,并采用激光粉末床熔化技术打印样品。采用 EBSD 手段进行表征并分析了晶粒尺寸的统计结果,从图 1~2 可以看出,

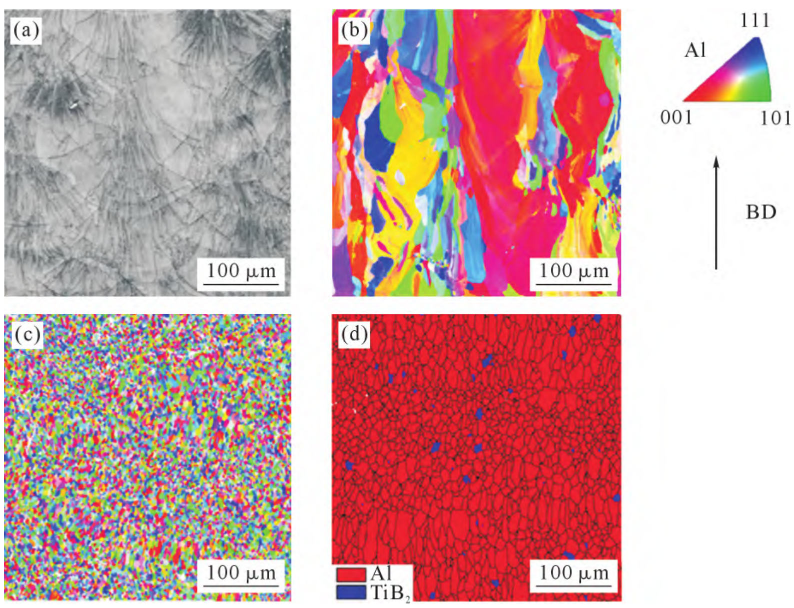

图 1 Al-Fe-Ni 和 TiB_2/Al-Fe-Ni 打印态样品 EBSD 结果:(a) Al-Fe-Ni 的 band contrast 图,(b) Al-Fe-Ni 的 IPF 图,(c) TiB_2/Al-Fe-Ni 的 IPF 图,(d) TiB_2/Al-Fe-Ni 的 TiB_2 相分布图[45]

Fig.1 EBSD results of the as-built Al-Fe-Ni alloy and TiB_2/Al-Fe-Ni composite samples: (a) band contrast map of the Al-Fe-Ni alloy, (b) inverse pole figure (IPF) map of the Al-Fe-Ni alloy, (c) IPF map of the TiB_2/Al-Fe-Ni composite, (d) local magnified phase map of the TiB_2/Al-Fe-Ni composite[45]

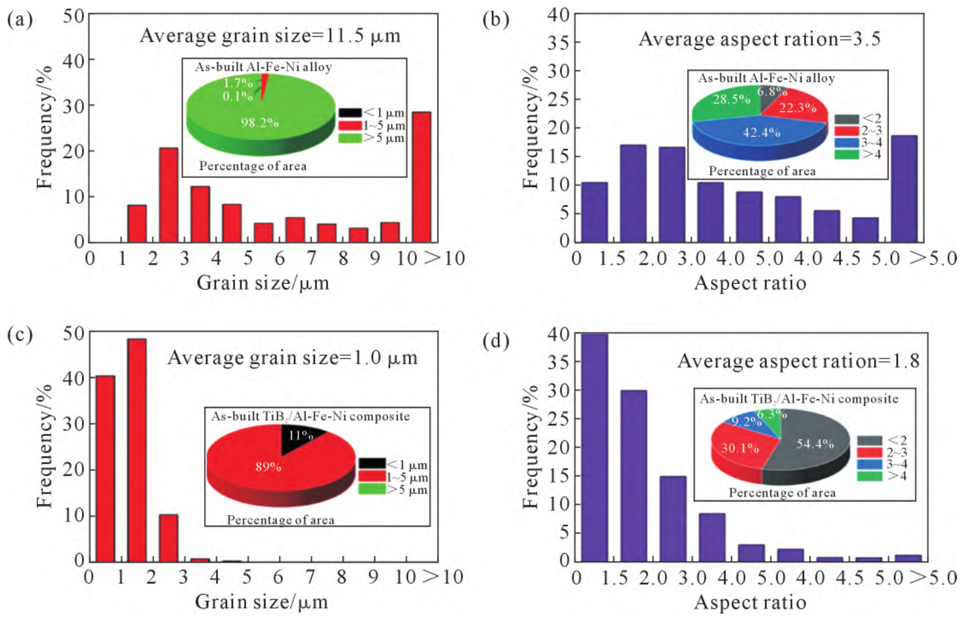

图 2　Al-Fe-Ni 和 TiB_2/Al-Fe-Ni 打印态样品晶粒尺寸和纵横比分布结果：(a~b) Al-Fe-Ni，(c~d) TiB_2/Al-Fe-Ni[45]

Fig.2　Grain size and aspect ratio distribution of the as-built Al-Fe-Ni alloy and TiB_2/Al-Fe-Ni composite samples: (a~b) Al-Fe-Ni alloy, (c~d) TiB_2/Al-Fe-Ni composite[45]

与 Al-Fe-Ni 打印态样品相比，TiB_2/Al-Fe-Ni 打印态样品的组织由粗大柱状晶转变为细小等轴晶，平均晶粒尺寸和晶粒纵横比分别减小 91%和 49%。上海交通大学 Sun 等[46]采用原位自生和气雾化法制备了 2%TiB_2/Al4Cu1.6Mg0.6Mn(质量分数)的复合粉末，应用激光粉末床熔化技术分别打印出 TiB_2/Al4Cu1.6Mg0.6Mn(A2T)和Al4Cu1.6Mg0.6Mn(A0T)样品。借助 EBSD 表征手段观察到沿着打印方向，与 A0T 打印态样品相比，A2T 打印态样品呈现出以细等轴晶为主加少量柱状晶的组织，平均晶粒尺寸减小 87%。TiB_2 纳米颗粒的引入使得铝合金的晶粒形态由柱状晶向等轴晶转变，细化了晶粒尺寸。

在铝合金打印态样品相对密度和可打印性的改变方面，Ding 等[45]的研究表明，打印态TiB_2/Al-Fe-Ni 具有更少和更小的圆形孔隙，打印态 TiB_2/Al-Fe-Ni 的最高相对密度要高于打印态 Al-Fe-Ni。所以，TiB_2/Al-Fe-Ni 的打印工艺窗口范围比 Al-Fe-Ni 合金更宽，可打印性更高[47]。Sun 等[46]的研究表明，A0T 打印态样品内部存在大量沿着打印方向的裂纹。如图3所示，在 250 W的激光功率下，扫描速度为 133 mm/s 和 83 mm/s 时，裂纹基本消失。而对于 A2T 打印态样品，在整个参数范围内，没有明显的裂纹，证明了 TiB_2/Al4Cu1.6Mg0.6Mn 具有更宽的打印工艺窗口。引入 TiB_2 改善了 Al4Cu1.6Mg0.6Mn合金在打印过

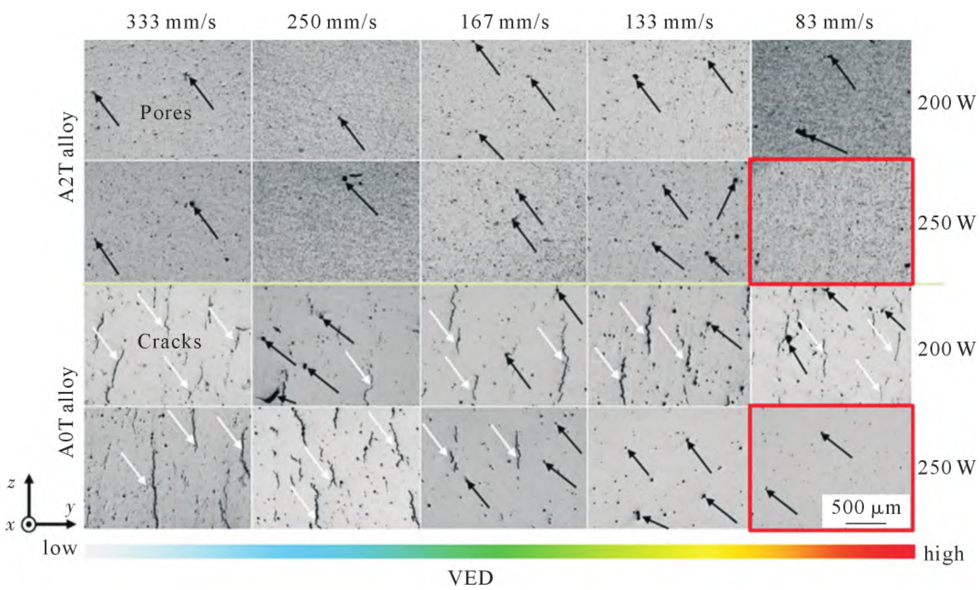

图 3　A2T 和 A0T 打印态样品在不同扫描速度和功率下沿着打印方向的 OM 图[46]

Fig.3　OM images of the as-built A2T and A0T samples with different scanning speeds and powers along the building direction[46]

程中的热裂纹问题,提高了可打印性。

在铝合金打印态样品力学性能的改变方面,Ding 等[45]、西北工业大学 Wang 等[48]、南京航空航天大学 Wang 等[49]、哈尔滨工业大学 Wang 等[14]分别对采用激光粉末床熔化技术打印的 TiB_2 增强铝基复合材料进行拉伸力学性能实验,结果如图 4 所示。图 4(a)表明,与 Al-Fe-Ni 打印态样品相比,TiB_2/Al-Fe-Ni 打印态样品的屈服强度、抗拉强度和伸长率分别提升 11.0%、10.6%、129.2%。图 4(b)表明,与打印态 2024Al 相比,打印态 TiB_2/2024Al 的屈服强度、抗拉强度和伸长率分别提升了 15.0%、24.4%、77.8%。图 4(c)表明,随着研磨剂量的增加,TiB_2/AlSi10Mg 复合材料的抗拉强度和伸长率先升高后降低, 只有 275 W·s/g 的研磨剂量使得 TiB_2/AlSi10Mg 打印态样品的抗拉强度和伸长率高于 AlSi10Mg 打印态样品。所以,采用球磨法制备铝基复合材料粉末时,需要考虑研磨剂量的影响, 选择合理的研磨剂量才能够提升铝合金的力学性能。图 4(d)表明,打印态 TiB_2/Al-Mg-Sc-Zr 的抗拉强度为(480±2) MPa,伸长率为(15.8±0.7)%,均高于打印态 Al-Mg-Sc-Zr。

综上所述,学者们对 TiB_2 纳米颗粒增强铝基复合材料的众多研究成果表明:①引入 TiB_2 纳米颗粒能够显著细化铝合金打印态样品的晶粒尺寸,促进柱状晶向等轴晶转变;②引入 TiB_2 纳米颗粒能够改善铝合金在激光粉末床熔化打印过程中出现的热裂纹和孔隙问题, 提升打印态样品的相对密度,拓宽了铝合金的激光粉末床熔化打印工艺窗口,提升了可打印性;③引入 TiB_2 纳米颗粒能够提升铝合金打印态样品的力学性能。但目前的研究并没有厘清不同牌号的铝合金,在不同引入方式下引入 TiB_2 纳米颗粒的含量和激光粉末床熔化打印工艺参数、打印态样品的相对密度、力学性能之间的复杂耦合关系。对于不同的铝合金,引入 TiB_2 纳米颗粒的最优含量以及相对密度和力学性能均能达到较好效果的打印参数仍有待进一步研究。

表 1 为总结的文献中一些 TiB_2 增强铝基复合材料的相关数据。

2 石墨烯增强

自 2004 年石墨烯成功从石墨中分离出来之后,石墨烯增强铝基复合材料的研究才得以不断由浅入深[54]。石墨烯与铝基体共格性良好,具有良好的导电性、导热性、惰性和表面性能[54],其独特的二维结构造就了优异的力学性能[55-56]。用于制备铝基复合材料的石墨烯包括氧化石墨烯(GO)和非氧化石墨烯(Gr)两大类, 石墨烯的形式主要有石墨烯纳米片(GNPs)和石墨烯粉末两种。制备石墨烯增强铝基复合材料的粉末主要有两种方法:球磨法和湿化学技术(异质团聚工艺)[54,57]。在研究之初,挤压铸造是用于制备石墨烯增强铝基复合材料的方法之一[58-59]。近年来学者们越来越关注采用激光粉末床熔化技术制备石墨烯增强铝基复合材料。引入石墨烯能够改变铝合金的激光吸收率,改变打印态样品的晶粒形态、晶粒尺寸、相对密度、可打印性和力学性能。

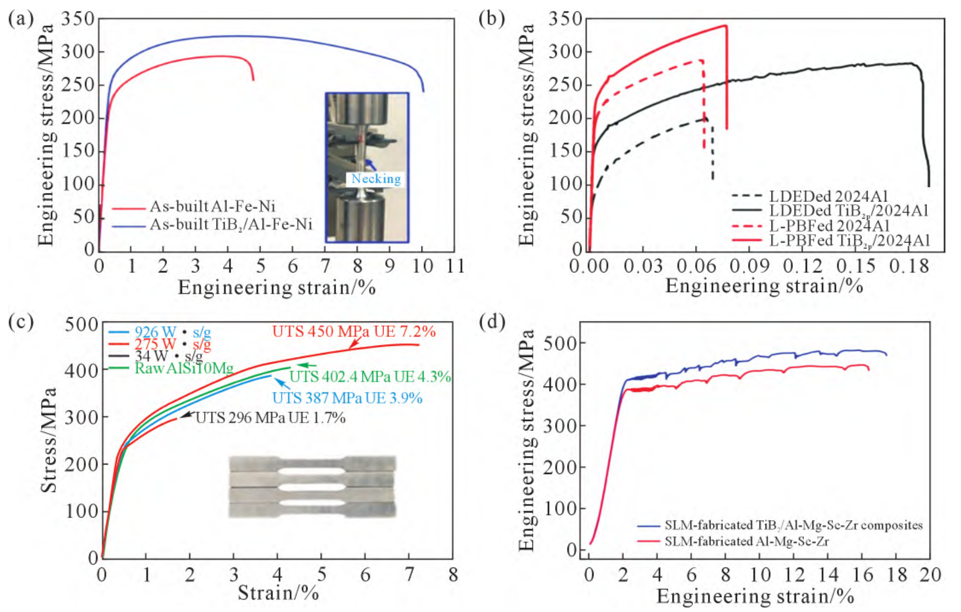

图 4 铝合金和 TiB_2 增强铝基复合材料打印态样品的工程应力-应变曲线:(a) Al-Fe-Ni 和 TiB_2/Al-Fe-Ni,(b) 2024Al 和 TiB_2/2024Al,(c) 不同研磨剂量制备的 TiB_2/AlSi10Mg,(d) Al-Mg-Sc-Zr 和 TiB_2/Al-Mg-Sc-Zr[14,45,48-49]

Fig.4 Engineering stress-strain curves of the as-built Al-alloys and TiB_2 reinforced aluminum matrix composites: (a) Al-Fe-Ni alloy and TiB_2/Al-Fe-Ni composite, (b) 2024Al and TiB_2/2024Al composite, (c) TiB_2/AlSi10Mg composite samples prepared from milled powder at different milling doses, (d) Al-Mg-Sc-Zr and TiB_2/Al-Mg-Sc-Zr[14,45,48-49]

表 1 TiB_2 增强铝基复合材料数据表("*"表示最大值)
Tab.1 Data sheet of TiB_2 reinforced aluminum matrix composites ("*" is maximum)

合金	引入 TiB_2 的方式	LPBF 打印参数 激光功率 P/W	扫描速度 v/(mm·s^{-1})	扫描间距 s/μm	层厚 t/μm	TiB_2 含量 w/%	相对密度 /%*	显微硬度 (HV)*	屈服强度 /MPa*	抗拉强度 /MPa*	伸长率 /%*	参考文献
Al-1.75%Fe-1.25%Ni (质量分数)	原位自生	225, 285	300~1800	90	30	0	99.28	-	244.5±4.2	293.5±2.4	4.8±0.5	[45]
						2%	99.89		271.3±2.3	324.7±0.9	11.0±1.1	
Al4Cu1.6Mg-0.6Mn	原位自生	200, 250	83, 133, 167, 250, 333	110	40	0	-	104±5.7	205.1±3.6	255.3±3.2	1.4±0.3	[46]
						2%		113.1±1.4	241.4±4.2	371.6±1.8	7.1±1.1	
2024Al	机械搅拌	280	100	100	30	0	-	-	206±1	270±13	4.5±1.6	[48]
						3%			237±6	336±25	8.0±2	
AlSi10Mg	原位自生	200	1 200	100	30	0	99.971	-	-	437.54±1.60	2.94±0.44	[50]
		210	1 000			5.6%	99.975			522.91±3.59	8.68±0.49	
AlSi10Mg	原位自生	220, 250, 280	800~2 000	90	30	0	99.56±0.16	125.9±1.4	270.1±4.3	430.7±1.6	4.7±0.4	[51]
						0.5%	99.82±0.10	140.5±1.3	317.6±2.1	484.1±3.3	9.5±0.3	
						2%	99.92±0.04	147.1±1.5	320.1±3.2	500.7±3.5	12.7±0.2	
						5%	99.91±0.02	151.1±2.1	323.7±1.9	522.9±3.6	8.7±0.5	
						8%	99.92±0.05	161.5±2.5	340.8±1.7	544.4±2.6	6.2±0.2	
AlSi10Mg	球磨法	450	1 600	50	50	0	99.34	-	-	402.4	4.3	[49]
						2%(研磨剂量 275 W·s/g)	99.15			450.0	7.2	
Al-7Si-Cu-Mg	原位自生	200	1 200	100	30	1.5%	-	-	297.2±0.2	474.6±1.8	13.4±0.5	[52]
AlCu-TiB_2 (A205)	-	250~300	-	90	30	-	99.5	-	317.8±9.3	391±7.3	12.5±0.8	[53]

日本东北大学 Dong 等[60]通过异质团聚工艺，制备出了质量分数为 0.3%氧化石墨烯(GO)/AlSi10Mg 粉末；Zhou 等[61]采用异质团聚工艺制备出 1.0%GO/Al(质量分数)粉末，均使用激光粉末床熔化技术打印样品。GO 中的 C 和 Al 在打印过程中发生反应，生成 Al_4C_3 强化相。借助 TEM 表征手段，从图 5(a)可以观察到，Al_4C_3 纳米相与基体紧密结合；图 5(b)显示出清晰的 Al_4C_3-Al 基体界面，该界面结合紧密，无中间化合物或纳米裂纹，表明 Al_4C_3-Al 界面能够进行有效的载荷传递，Al_4C_3 纳米相具有良好的承载能力，能够对基体起到强化作用。在铝合金激光吸收率的改变方面，图 6 表明，GO 的激光吸收率高于 AlSi10Mg 和纯 Al，因而引入 GO 增强了 AlSi10Mg 和纯 Al 的激光吸收率，使得 AlSi10Mg 和纯 Al 的可打印性得到提升。

在铝合金打印态样品晶粒形态和尺寸的改变方面，印度博帕尔先进材料与工艺研究所 Tiwari 等[62]采用球磨法制备出石墨烯(Gr)/AlSi10Mg 粉末，通过激光粉末床熔化技术打印样品。图 7 的 EBSD 结果表明，沿着打印方向，随着石墨烯含量增加，Gr/AlSi10Mg 的组织出现了更多的细小等轴晶，平均晶粒尺寸减小(表 2)。中北大学 Zhao 等[63]采用有机铝化学还原和球磨法制备出 1%Al(质量分数)包覆石墨烯(Al-coated Gr)/AlSi10Mg 复合粉末，使用激光粉末床

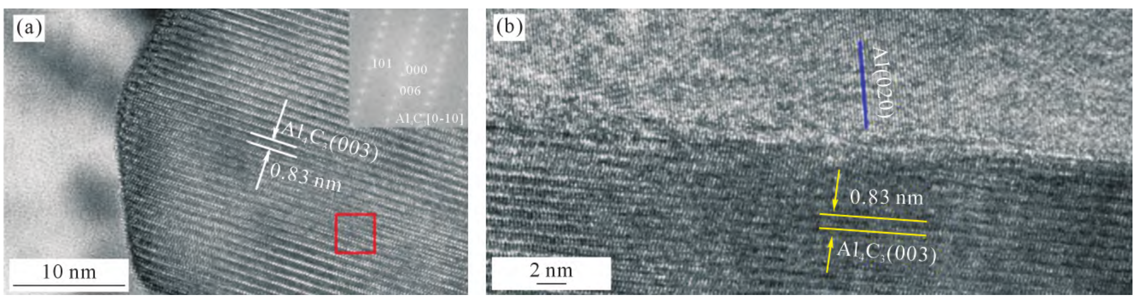

图 5 石墨烯增强铝基复合材料打印态样品 Al_4C_3-Al 界面的 HRTEM 图像：(a) GO/AlSi10Mg，(b) GO/Al[60-61]
Fig.5 HRTEM images of the Al_4C_3-Al interface in as-built graphene reinforced aluminum matrix composite: (a) GO/AlSi10Mg, (b) GO/Al[60-61]

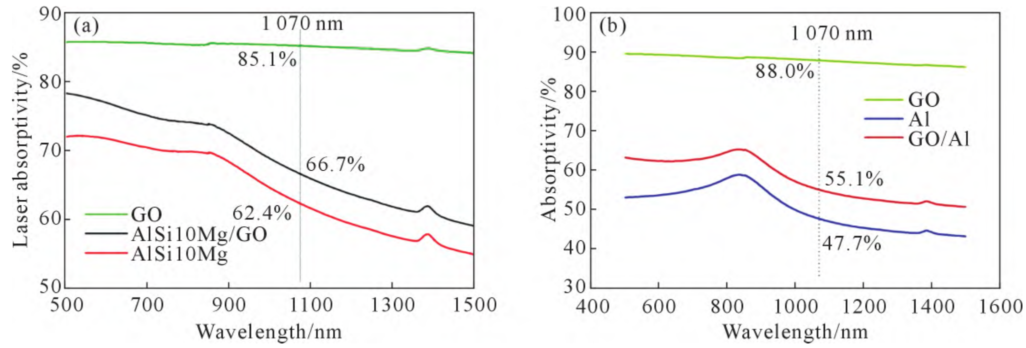

图 6 在 500~1 500 nm 波长范围内的激光吸收率随波长的变化:(a) GO/AlSi10Mg,(b) GO/Al[60-61]

Fig.6 Laser absorptivity as a function of wavelength in the range of 500~1 500 nm: (a) GO/AlSi10Mg, (b) GO/Al[60-61]

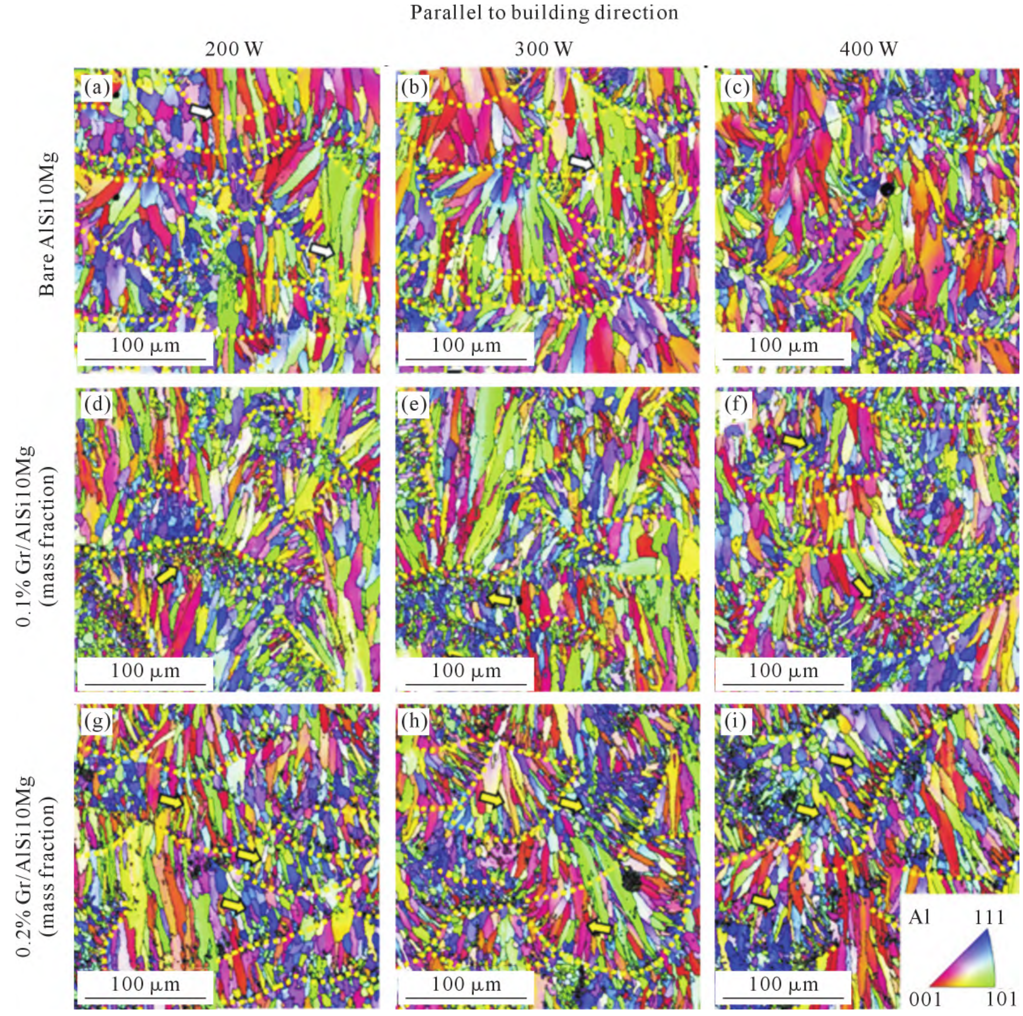

图 7 AlSi10Mg 和 Gr/AlSi10Mg 打印态样品在不同打印参数下沿着打印方向的 IPF 图[62]

Fig.7 IPF maps of the as-built AlSi10Mg and Gr/AlSi10Mg samples along the building direction at different print parameters[62]

表 2 合金样品和复合样品沿着打印方向上的平均晶粒尺寸[62]

Tab. 2 Average grain size of bare and composite samples along the building direction[62]

材料	平均晶粒尺寸 /μm		
	200 W	300 W	400 W
AlSi10Mg	13.47±3.14	14.25±3.45	12.29±3.01
0.1%Gr/AlSi10Mg(质量分数)	9.56±2.84	10.97±2.80	10.10±2.94
0.2%Gr/AlSi10Mg(质量分数)	8.12±2.17	9.15±2.59	8.73±2.64

熔化技术打印样品。图 8 表明,在 AlSi10Mg 合金中引入 Al 包覆石墨烯后,粗晶胞数量减少,形成了更多的细球形晶胞。

在铝合金打印态样品相对密度、可打印性以及力学性能的改变方面,Tiwari 等[62]的研究结果如图 9 所示,当激光功率为 300 W 时,AlSi10Mg 的打印态样品孔隙较少;当激光功率增加到 400 W 时,质量分数为 0.1%和 0.2%石墨烯增强样品的孔隙相对较少,复合粉末熔融情况良好。这说明引入石墨烯后,复合材料的打印参数需要进一步优化,且相对密度并非随着石墨烯含量增加而增加。美国辛辛那提大

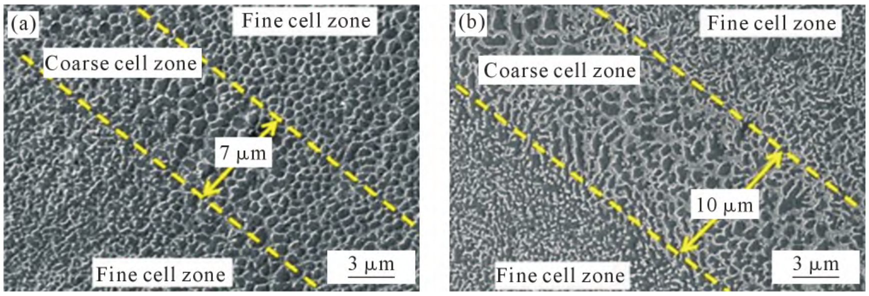

图 8　打印态样品显微照片：(a) Al 包覆石墨烯 /AlSi10Mg 复合材料的微观结构(横截面)，(b) AlSi10Mg 合金的微观结构(横截面)[63]

Fig.8　Micrographs of the as-built samples: (a) Al-coated Gr/AlSi10Mg composite (cross section), (b) AlSi10Mg alloy (cross section)[63]

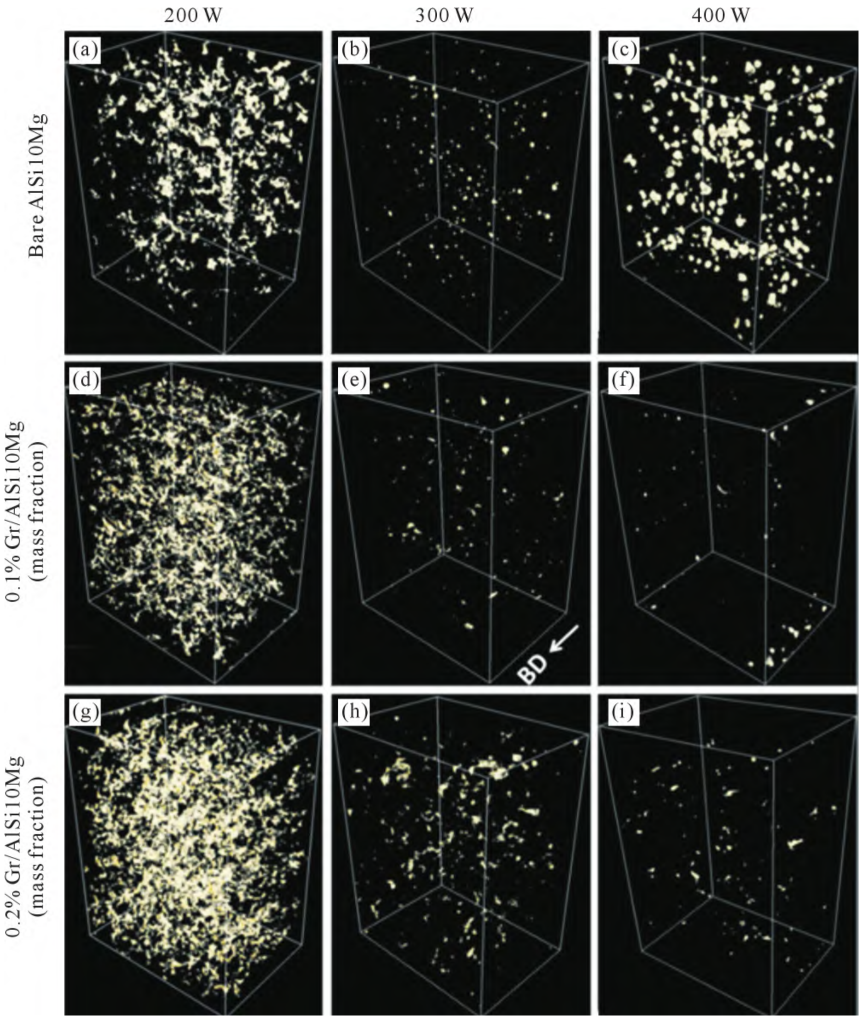

图 9　在不同激光功率下制备的合金样品和复合样品中孔隙的体积分布[62]

Fig.9　Volumetric distribution of pores in alloy and composite samples prepared at various laser powers[62]

学 Wang 等[64]采用球磨法制备出 0.5%(质量分数)石墨烯纳米片(GNPs)/AlSi10Mg 粉末，通过激光粉末床熔化技术用相同打印参数打印 AlSi10Mg 样品和 GNPs/AlSi10Mg 样品。图 10 表明，GNPs/AlSi10Mg 打印态样品的相对密度低于 AlSi10Mg 打印态样品，但 GNPs/AlSi10Mg 的屈服强度、抗拉强度、伸长率高于 AlSi10Mg。说明引入 0.5%石墨烯(质量分数)对打印态 AlSi10Mg 产生了强化效果，但要提高 GNPs/AlSi10Mg 打印态样品的相对密度仍需要进一步优化打印参数。Tiwari 等[62]、Zhao 等[63]、Zhou 等[61]分别对采用激光粉末床熔化技术打印的石墨烯增强铝基复合材料进行相关力学性能实验，结果如图 11 所示。从图 11(a~c)及(f)可以看到，0.1% Gr/AlSi10Mg(质量分数)打印态样品的屈服强度和抗拉强度最佳，AlSi10Mg 合金的打印态样品的伸长率最好。打印态样品的力学性能是由石墨烯的引入和样品的相对密度共同作用，并非引入石墨烯的含量越高，力学性能越好。但 AlSi10Mg 打印态样品的显微硬度随着石墨烯引入量增加而增加。如图 11 (d)所示，Al-coated Gr/AlSi10Mg 打印态样品的抗拉强度

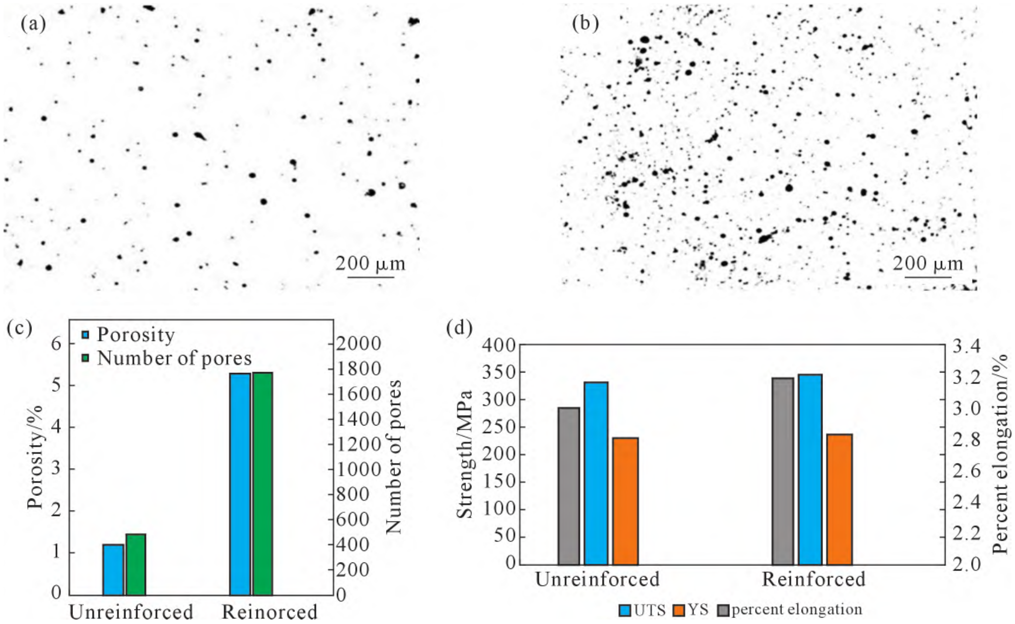

图 10 打印态样品的孔隙分析和拉伸性能：(a) 打印态 AlSi10Mg 中孔隙的显微照片，(b) 打印态 GNPs/AlSi10Mg 中孔隙的显微照片，(c) 孔隙率比较，(d) 拉伸性能[64]

Fig.10 Pore analysis and tensile performance of the as-built samples: (a) micrographs of pores in AlSi10Mg, (b) micrographs of pores in GNPs/AlSi10Mg, (c) porosity comparison, (d) tensile performance[64]

为 396 MPa，伸长率为 6.2%。Al-coated Gr/AlSi10Mg 打印态样品的显微硬度为 169 HV。其抗拉强度、伸长率、显微硬度均高于 AlSi10Mg 打印态样品。如图 11(e)所示，可以看到 GO/Al 打印态样品(即图中的 Al_4C_3/Al) 的横纵截面的显微硬度要高于纯 Al，进一步证明了 GO/Al 在打印过程中生成的弥散分布的棒状 Al_4C_3 纳米相具有良好强化效果。Zhao 等[63]的摩擦实验结果如图 12 所示，打印态 Al-coated Gr/AlSi10Mg 平均摩擦系数为 0.274，低于打印态 AlSi10Mg 的 0.472，说明打印态 Al-coated Gr/AlSi10Mg 的耐磨性优于打印态 AlSi10Mg 合金。Wu 等[65]同样用实验证明了打印态 GNPs/AlSi10Mg 复合材料的耐磨性更好。打印态 AlSi10Mg 的显微硬度为 119 HV，GNPs/AlSi10Mg 的显微硬度为 174 HV。即

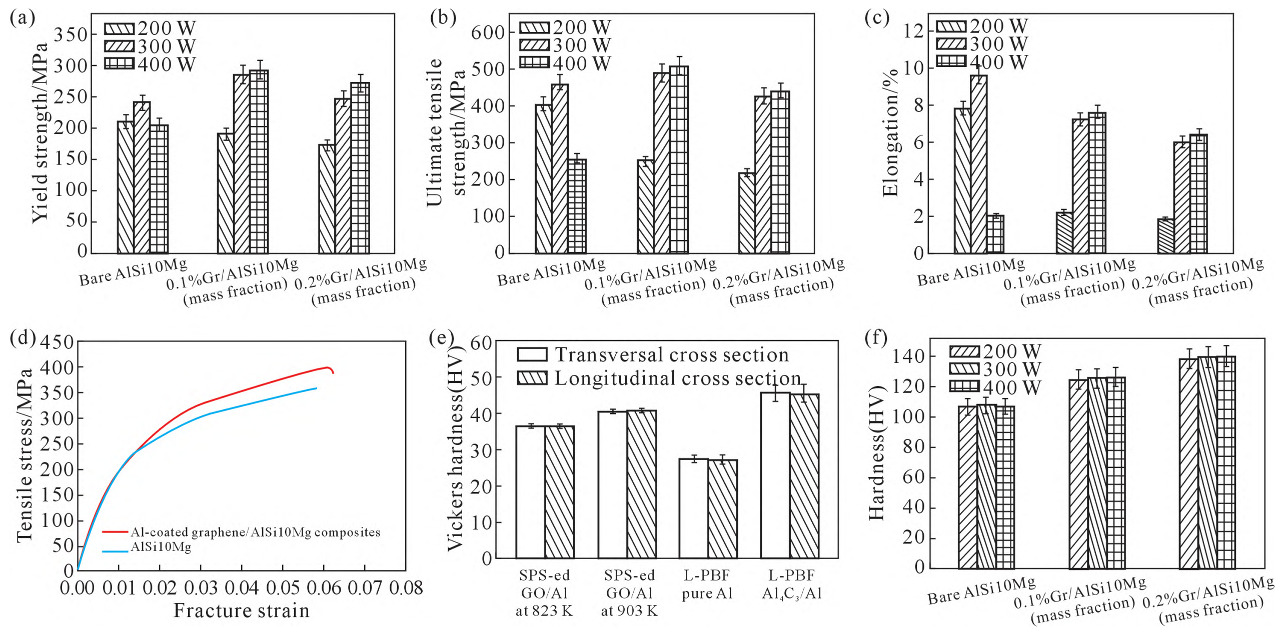

图 11 打印态样品的相关力学性能实验结果：(a~c) AlSi10Mg 和 Gr/AlSi10Mg 的屈服强度，抗拉强度和伸长率，(d) AlSi10Mg 和 Al 包覆石墨烯 /AlSi10Mg 的工程应力−应变曲线，(e) Al、Al_4C_3/Al 的横纵截面显微硬度，(f) AlSi10Mg 和 Gr/AlSi10Mg 的显微硬度[61-63]

Fig.11 Experimental results of mechanical properties related to the as-built samples: (a~c) yield strength, tensile strength and elongation of AlSi10Mg and Gr/AlSi10Mg, (d) engineering stress-strain curves of AlSi10Mg and Al-coated Gr/AlSi10Mg, (e) microhardness of Al and Al_4C_3/Al composite in the transversal and longitudinal cross sections, respectively, (f) microhardness of AlSi10Mg and Gr/AlSi10Mg[61-63]

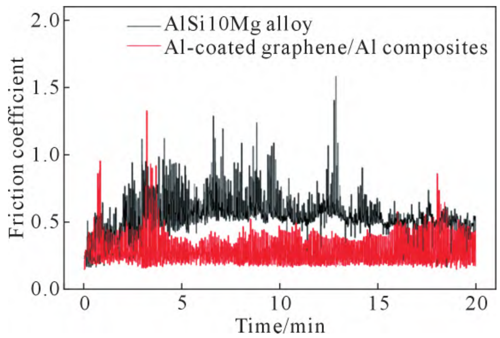

图 12 摩擦系数与时间的曲线[63]
Fig.12 The curves of the friction coefficient and time[63]

显微硬度高的铝基复合材料具有良好的耐磨性[66]。

综上所述，学者们对石墨烯增强铝基复合材料的众多研究成果表明：①引入石墨烯能够提高铝及铝合金的激光吸收率，提升可打印性；②引入石墨烯能够细化铝合金打印态样品的晶粒尺寸，提高显微硬度和耐磨性。但目前的研究结果仍有不完善之处：铝基复合材料的相对密度和拉伸力学性能并非随着引入石墨烯含量的增加而提升，需要综合考虑打印参数的影响。为了使得石墨烯增强铝基复合材料的打印态样品能达到较优强化效果，对于不同牌号的铝合金，引入石墨烯的含量、打印参数和最终打印态样品的相对密度、力学性能之间的相互作用关系，仍有待进一步研究。

表 3 为总结的文献中一些石墨烯增强铝基复合材料的相关数据。

3　TiC 增强

TiC 具有高硬度、高弹性模量、良好润湿性、良好激光吸收率等优点[67-68]。TiC 纳米颗粒引入铝及铝合金的方式以外加法(球磨法、超声搅拌法等)为主。起初，超声辅助搅拌铸造、喷雾沉积、粉末冶金等是用于制备 TiC 纳米颗粒增强铝基复合材料的主要工艺[69-74]。近年来由于增材制造技术的不断应用和推广，TiC 纳米颗粒增强铝基复合材料的生产工艺得以逐步向以激光粉末床熔化为代表的增材制造技术过渡和发展。引入 TiC 纳米颗粒能够改变铝合金打印态样品的晶粒形态、晶粒尺寸、相对密度、可打印性和力学性能。

在铝合金打印态样品晶粒形态和尺寸的改变方面，南昌航空大学 Fan 等[75]采用球磨法使得 TiC 纳米颗粒均匀分布在 AA2024 铝合金粉末表面，制成了 TiC/AA2024 复合粉末，并采用激光粉末床熔化技术打印样品。经过 EBSD 分析表征，发现随着引入 TiC 纳米颗粒含量的增加，能够细化打印态 AA2024 铝合金的晶粒尺寸，促进柱状晶向等轴晶的转变。山东大学贾增庆等[76]使用真空感应气雾化方法制备出了 AlSi10Mg 合金 +2024 铝合金 +1.5% TiC(质量分数)的复合粉末，命名为 AlSi10Mg-2024 (TiC)，并采用激光粉末床熔化技术打印样品。图 13 为打印态样品沿着打印方向的 EBSD 结果，从图 13 (a~b) 对比可以看出，TiC 纳米颗粒起到了细化晶粒和促进柱状晶向等轴晶转变的作用，并有效改善了打印态样品的各向异性。美国辛辛那提大学 Wang 等[77]将 AlSi10Mg 粉末和 TiC 纳米颗粒通过湿球磨和超声搅拌的方式进行混合，得到 3.0% TiC/AlSi10Mg(质量分数)复合粉末，并采用激光粉末床熔化技术打印样品。研究表明，引入 TiC 纳米颗粒会细化 AlSi10Mg 打印态样品的晶粒尺寸，促进柱状

表 3 石墨烯增强铝基复合材料数据表(“*”表示最大值)
Tab.3 Data sheet of graphene reinforced aluminum matrix composites (“*” is maximum)

基体	引入石墨烯的方式	LPBF 打印参数 激光功率 P/W	扫描速度 v/(mm·s^{-1})	扫描间距 s/μm	层厚 t/μm	石墨烯含量 w/%	相对密度 /%*	显微硬度 (HV)*	屈服强度 /MPa*	抗拉强度 /MPa*	伸长率 /%*	参考文献
AlSi10Mg(引入氧化石墨烯)	异质团聚工艺	95	150~350	45~105	30	0 0.3%	-	95 100.6	-	-	-	[60]
AlSi10Mg(引入非氧化石墨烯)	球磨法	200 300 400	2250	90	30	0 0.1% 0.2%	99.2 99.2 98.3	如图 11(a)、(b)、(c)、(f)所示				[62]
AlSi10Mg(引入非氧化石墨烯纳米片)	球磨法	370	1300	190	30	0 0.5%	-	-	234 246	337 346	3.0 3.2	[64]
AlSi10Mg(引入 Al 包覆石墨烯)	球磨法	200~400	1200	130	30	0 1%	- 98	120 169	-	357 396	5.5 6.2	[63]
AlSi10Mg(引入非氧化石墨烯纳米片)	球磨法	300 330	-	130 140	30	0 0.5%	-	119 174	-	-	-	[65]
Al(引入氧化石墨烯)	异质团聚工艺	20.6	10	100	25	0 1.0	97.12 97.36	27.4 45.6	-	-	-	[61]

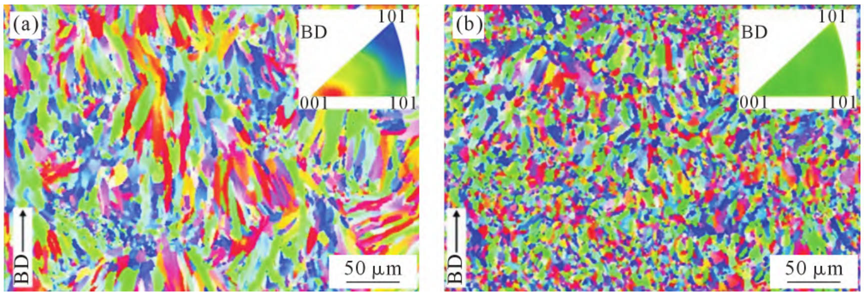

图 13 沿打印方向 IPF 图:(a) AlSi10Mg 合金,(b) AlSi10Mg-2024 (TiC)[76]
Fig.13 IPF maps along the building direction: (a) AlSi10Mg alloy, (b) AlSi10Mg-2024 (TiC)[76]

晶向等轴晶转变。

在铝合金打印态样品相对密度、可打印性的改变方面,Fan 等[75]对打印态样品的相对密度和裂纹分析如图 14~15 所示，在激光扫描速度为 600~1 500 mm/s 的工艺窗口下,未引入 TiC 纳米颗粒的 AA2024 铝合金打印态样品的热裂纹面积分数较大。随着引入的 TiC 纳米颗粒含量增加，热裂纹面积分数减小，样品相对密度逐渐增加,说明引入 TiC 纳米颗粒提升了 AA2024 铝合金的可打印性。在铝合金打印态样品力学性能的改变方面,贾增庆等[76]、Wang 等[77]分别对采用激光粉末床熔化技术打印的 TiC 增强铝基复合材料进行相关力学性能实验，实验结果如图 16 所示。贾增庆等[76]的实验结果(图 16(a~b))表明,AlSi10Mg-2024(TiC)打印态样品的显微硬度、屈服强度和抗拉强度相较于 AlSi10Mg 合金均有所提高。Wang 等[77]的研究(图 16(c~d))发现,3.0% TiC/AlSi10Mg(质量分数)打印态样品的屈服强度和抗拉强度均高于 AlSi10Mg 打印态样品，但是 Al-

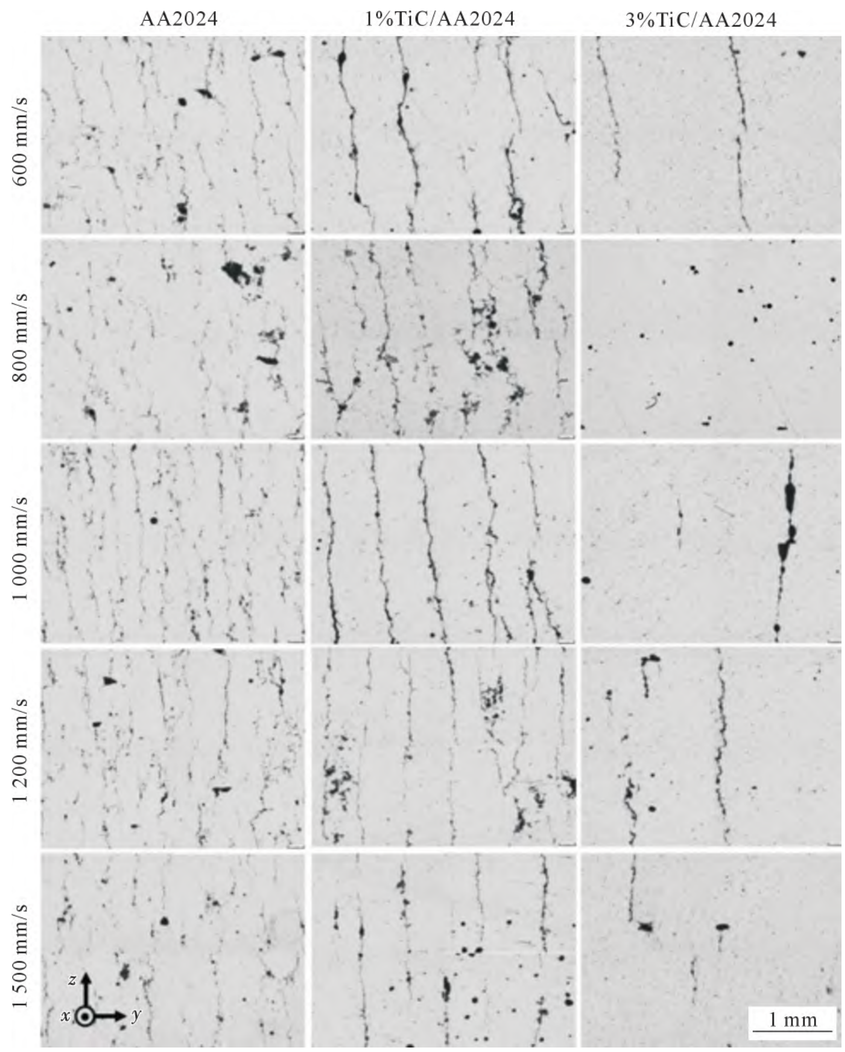

图 14 不同激光功率打印态合金和复合样品 OM 图[75]
Fig.14 OM images of the as-built alloy and composite samples at various laser powers[75]

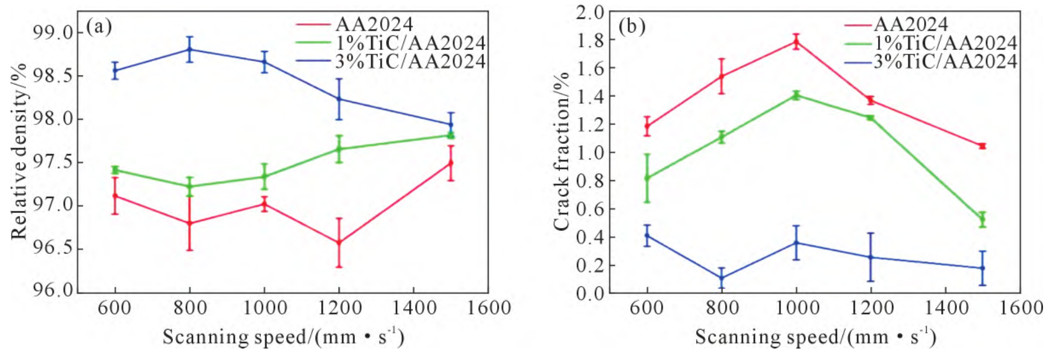

图 15 打印态样品相对密度和裂纹分析:(a) AA2024 铝合金和复合样品的相对密度和扫描速度的关系,(b) AA2024 铝合金和复合样品裂纹面积分数和扫描速度的关系[75]

Fig.15 Relative density and crack analysis of the as-built samples: (a) the relative density of AA2024 Al alloy and composite at different laser scanning speeds, (b) the area fraction of cracks in AA2024 Al alloy and composite at different laser scanning speeds[75]

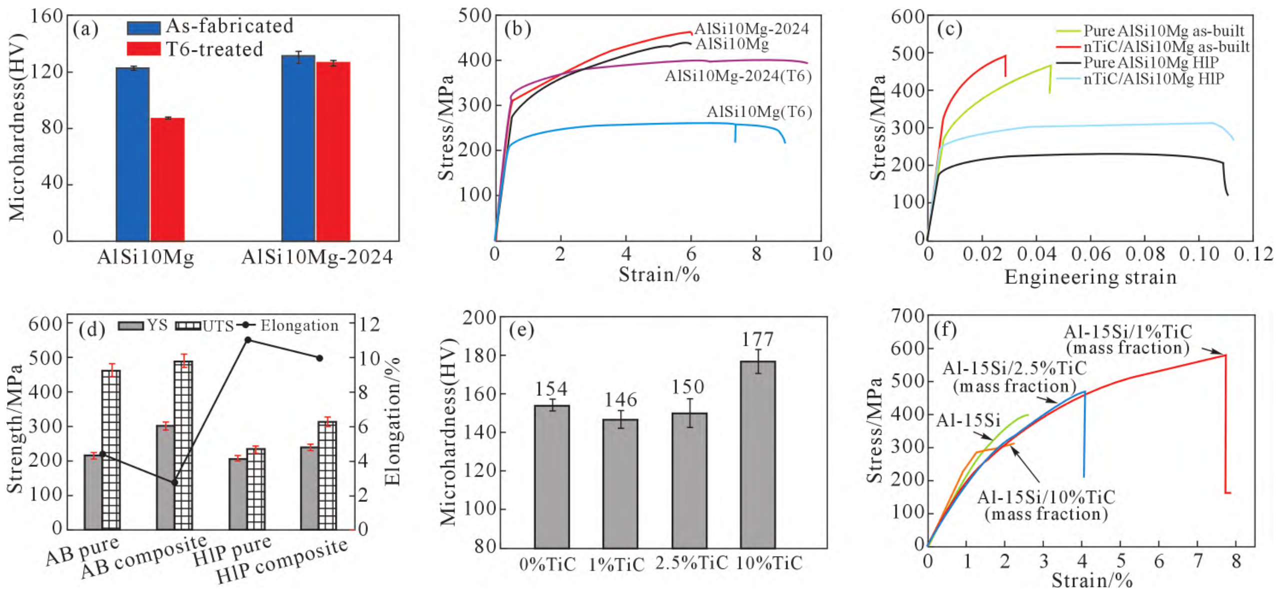

图 16 打印态样品的相关力学性能实验结果:(a~b) 打印态和 T6 热处理后 AlSi10Mg 和 AlSi10Mg-2024(TiC)的显微硬度及工程应力-应变曲线,(c~d) AlSi10Mg 和 TiC/AlSi10Mg 的工程应力-应变曲线及屈服强度、抗拉强度、伸长率的比较,(e~f) Al-15Si 和 TiC/Al-15Si 的显微硬度及工程应力-应变曲线[76-78]

Fig.16 Experimental results of mechanical properties related to the as-built samples: (a~b) microhardness and engineering stress-strain curves of AlSi10Mg and AlSi10Mg-2024(TiC) both in as-built condition and after T6 heat treatment, (c~d) engineering stress-strain curves and comparison of yield strength, tensile strength, elongation of AlSi10Mg and TiC/AlSi10Mg, (e~f) microhardness and engineering stress-strain curves of Al-15Si and TiC/Al-15Si[76-78]

Si10Mg 打印态样品的伸长率更高。中国地质大学(武汉)Zhou 等[78]采用球磨法分别制备出了质量分数为 1%、2.5%、10%TiC/Al-15Si 复合粉末，通过激光粉末床熔化技术打印样品，并进行了相关力学性能测试。从图 16(e~f)可以看出,随着 TiC 含量增加,TiC/Al-15Si 的显微硬度先减小后增大;抗拉强度和伸长率先增大后减小。

综上所述,学者们对 TiC 纳米颗粒增强铝基复合材料的众多研究成果表明:①引入 TiC 纳米颗粒能够细化铝合金打印态样品的晶粒尺寸，增加细等轴晶比例;②引入 TiC 纳米颗粒能够改善铝合金的热裂纹缺陷，提高可打印性。但目前的研究仍然有待完善:引入 TiC 纳米颗粒并不一定能够提升铝合金打印态样品的显微硬度和拉伸力学性能,TiC 纳米颗粒增强铝基复合材料的力学性能是一个由 TiC 纳米颗粒含量、激光粉末床熔化打印参数、铝基复合材料的组织、打印态样品相对密度等因素共同作用和影响的结果，之间的复杂关系仍然需要进行进一步研究。

表 4 为总结的文献中一些 TiC 增强铝基复合材料的相关数据。

4 不同纳米增强体对打印态铝合金力学性能影响的对比

近年来，关于向铝合金中引入的纳米增强体层出不穷,主要分为五大类:硼化物、碳单质、碳化物、氮化物、金属氧化物。除了本文提到的 TiB_2、石墨烯、TiC,还有 LaB_6[80]、CaB_6[81]、金刚石[82]、SiC[83-85]、B_4C[86]、

表 4 TiC 增强铝基复合材料数据表("*"表示最大值)

Tab. 4 Data sheet of TiC reinforced aluminum matrix composites ("*" is maximum)

合金	引入 TiC 的方式	LPBF 打印参数 激光功率 P/W	扫描速度 v/ mm·s^{-1}	扫描间距 s/μm	层厚 t/μm	TiC 含量 w/%	相对密度 /%*	显微硬度 (HV)*	屈服强度 /MPa*	抗拉强度 /MPa*	伸长率 /%*	参考文献
AlSi10Mg-2024(TiC)	-	275	-	80	40	0	-	122	285±10	435±5	均为 5~6	[76]
						1.5%		130	300±21	451±12		
AlSi10Mg	湿球磨和超声搅拌	250	400	45	25	0	-	-	216.8	464.2	4.4	[77]
						3%			302.0	489.7	-	
AlSi10Mg	球磨法	100	100,143 200,400	50	50	5%	>98	177.6	-	-	-	[79]
Al-15Si	球磨法	360	600,650	60	20	0	-	154	-	398	2.6	[78]
						1%		146		578	7.86	
						2.5%		150		-	-	
						10%		177		313	2.24	

Al_4SiC_4[87]、AlN[88-89]、TiN[90]、TiCN[91]、Si_3N_4[92]、BN[93]、Fe_3O_4[28]、$MgAl_2O_4$[94]等。这些纳米增强体对打印态铝合金力学性能的改善可归结为以下两大机理：①引入的纳米增强体能够作为异质形核位点，促进激光粉末床熔化打印凝固过程中的晶粒形核，形成更多细小等轴晶，细化晶粒尺寸，产生细晶强化；②引入的纳米增强体会形成弥散分布的第二相粒子，产生第二相强化。为了直观反映出现有主流纳米增强体对打印态铝合金力学性能改变的分布情况，结合文献中的数据，作出了图 17。

从图 17(a)可以看出，对于打印态 AlSi10Mg，引入 TiB_2 能够使其抗拉强度和伸长率都得到提高；引入 LaB_6 对其伸长率提高较大，但抗拉强度变化不明显；引入 TiC 和 Si_3N_4 对其抗拉强度有一定提高作用，但伸长率出现了下降的现象；而其他纳米增强体效果不理想，甚至出现了抗拉强度降低的现象。因此，TiB_2 纳米颗粒的引入对于打印态 AlSi10Mg 来说效果非常良好，对强塑性均有提升的作用。从图 17(b)可以看出，对于其他牌号的打印态铝合金，引入相应的纳米增强体都实现了抗拉强度和伸长率的一定提高。如图 17(c)所示，除了 AlN，其余纳米增强体都能够提高打印态 AlSi10Mg 的显微硬度。如图 17(d)所示，对于其他牌号的打印态铝合金，引入相应的纳米增强体对显微硬度都有所提高。

综上所述，以 TiB_2 为代表的纳米增强体对打印态铝合金的强化效果良好，能够起到强度、塑性均有

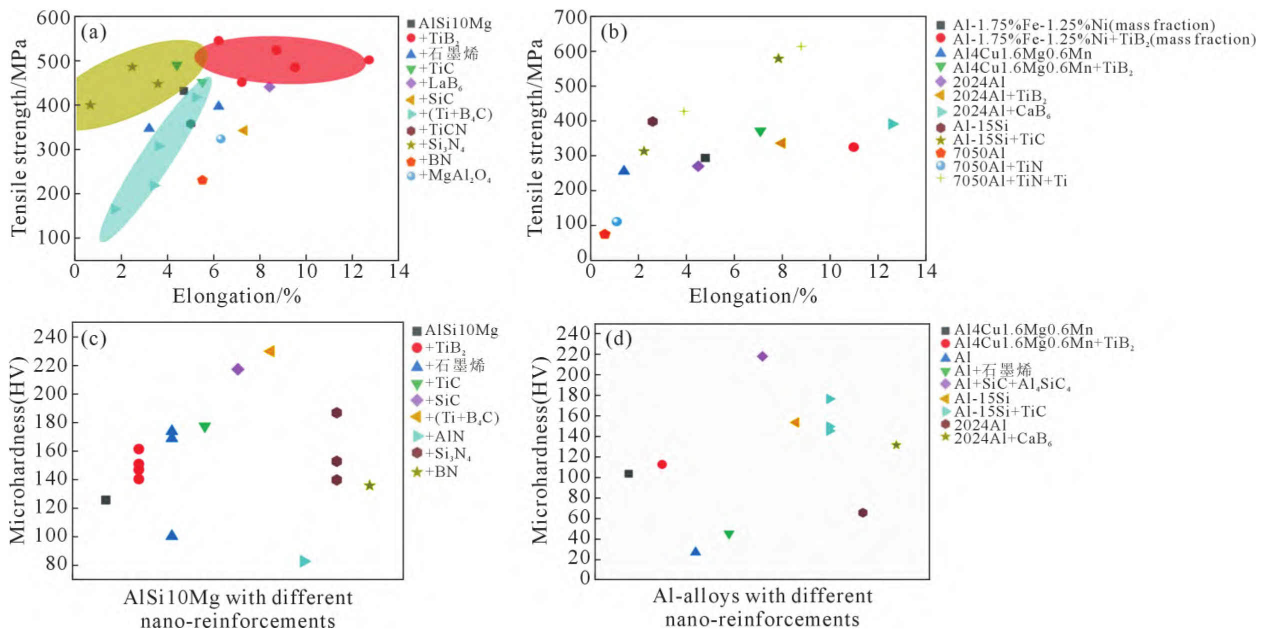

图 17 不同纳米增强体对打印态铝合金力学性能改变的对比：(a~b) AlSi10Mg 及其他铝合金抗拉强度和伸长率，(c~d) AlSi10Mg 及其他铝合金显微硬度[45-46,48,51,60-61,63-65,76-81,84,86-87,89-94]

Fig.17 Comparison of different nano-reinforcements on the change in the mechanical properties of the as-built aluminum alloys: (a~b) tensile strength and elongation of AlSi10Mg and other Al-alloys, (c~d) microhardness of AlSi10Mg and other Al-alloys[45-46,48,51,60-61,63-65,76-81,84,86-87,89-94]

提升的效果。但不同牌号铝合金强化效果最佳的纳米增强体种类及引入的含量仍需要再进一步研究。

5 结论

(1)在铝合金中引入 TiB_2、石墨烯、TiC 纳米增强体所制备出的铝基复合材料，能够提高铝合金的激光吸收率；促进组织中的粗大柱状晶向细等轴晶转变，细化晶粒尺寸；改善铝合金在激光粉末床熔化加工过程中的热裂纹缺陷，提升可打印性。

(2)在铝合金中引入 TiB_2、石墨烯、TiC 纳米增强体能够调整材料的力学性能，但铝合金力学性能的改变并非和引入纳米增强体的含量呈简单的正相关关系。同样，铝基复合材料的相对密度也并不一定随着引入纳米增强体含量的增加而增加。铝基复合材料的力学性能是一个由纳米增强体含量、激光粉末床熔化打印参数、铝基复合材料的组织、打印态样品相对密度等因素共同作用的复杂结果。

(3)原位自生引入 TiB_2 纳米颗粒的方式能够获得均匀的颗粒分布，且在原材料制备阶段即引入强化颗粒相，减少了球磨混合的工序，适合批量化增材制造应用。

6 前景展望

(1)针对于不同牌号的铝合金和种类繁多的纳米增强体，每种铝合金对应引入何种纳米增强体能够起到相对较优的缺陷改善效果和可打印性、力学性能等性能的提升，是有待进一步研究的问题。

(2)在航空航天、军工、交通运输等领域所用到的铝基复合材料关键部件需要重点关注其力学性能的优劣和相对密度的高低问题。打印态铝基复合材料的力学性能和相对密度并不一定随着纳米增强体含量的增加而提升，还需要综合考虑激光粉末床熔化的最优打印工艺参数的问题。因此，能否建立不同种类铝基复合材料的力学性能、相对密度和激光粉末床熔化打印工艺参数及引入纳米增强体含量的定量关系极为关键，具有很大研究前景，若能针对具体情况给出数值模拟计算模型作为铝基复合材料力学性能的预测，则能够提高设计实验研究方案和制定加工参数的效率。

(3)为了阐明纳米增强体在激光粉末床熔化打印过程中发生的现象和变化，数值模拟和实验方法需要进一步发展。因此，通过建立相关物理模型对纳米增强体在熔池中的行为进行数值模拟，并采用 X 射线同步辐射对打印过程进行原位观测，可以帮助深入理解内在机理并更好地进行打印工艺参数的优化。

(4)热等静压(hot isostatic pressing，HIP)能够起到焊合打印态样品裂纹的作用，但其高温环境会造成铝基复合材料的晶粒尺寸有所增加。因此，能否采用 HIP 来帮助改善热裂纹缺陷，并对力学性能产生较小的影响是有待进一步研究的问题。

(5)采用激光粉末床熔化技术制备的铝基复合材料会在未来释放更大潜力，推动航空航天、军工、交通运输等行业进一步发展。

参考文献：

[1] 房豪杰，曲华，杨黎晖，等. 9C 系列粉末冶金高耐蚀铝合金腐蚀行为研究[J]. 中国腐蚀与防护学报，2021, 41(6): 775-785.
FANG H J, QU H, YANG L H, et al. Corrosion behavior of 9C series of powder metallurgy Al-alloy with high corrosion resistance [J]. Journal of Chinese Society for Corrosion and Protection, 2021, 41(6): 775-785.

[2] 马晓波，王东新，胡侨丹，等. 元素添加强化铍铝合金研究现状[J]. 稀有金属，2021, 45(8): 1010-1017.
MA X B, WANG D X, HU Q D, et al. Research status of additive elements to strengthen beryllium aluminum alloy[J]. Chinese Journal of Rare Metals, 2021, 45(8): 1010-1017.

[3] SUN T T, WANG H Z, GAO Z Y, et al. The role of in-situ nano-TiB_2 particles in improving the printability of noncastable 2024Al alloy[J]. Materials Research Letters, 2022, 10(10): 656-665.

[4] SUN T T, CHEN J, WU Y, et al. Achieving excellent strength of the LPBF additively manufactured Al-Cu-Mg composite via in-situ mixing TiB_2 and solution treatment [J]. Materials Science and Engineering: A, 2022, 850: 143531.

[5] 齐世文，荣鹏，黄丹，等. 激光粉末床熔融增材制造铝合金的室温和高温力学性能研究[J]. 中国激光，2022, 49(8): 7-17.
QI S W, RONG P, HUANG D, et al. Room- and high-temperature mechanical properties of aluminum alloys fabricated using laser powder bed fusion additive manufacturing[J]. Chinese Journal of Lasers, 2022, 49(8): 7-17.

[6] 胡娟，高银涛，冒浴沂，等. 激光粉末床熔融金属制件孔隙缺陷研究现状[J]. 粉末冶金工业，2021, 31(6): 87-93.
HU J, GAO Y T, MAO Y Y, et al. Research progress of pore defects for metal parts manufactured by laser powder bed fusion[J]. Powder Metallurgy Industry, 2021, 31(6): 87-93.

[7] XIAO Y K, BIAN Z Y, WU Y, et al. Simultaneously minimizing residual stress and enhancing strength of selective laser melted nano-TiB_2 decorated Al alloy via post-uphill quenching and ageing [J]. Materials Characterization, 2021, 178: 111242.

[8] DING H, XIAO Y K, BIAN Z Y, et al. Design, microstructure and thermal stability of a novel heat-resistant Al-Fe-Ni alloy manufactured by selective laser melting[J]. Journal of Alloys and Compounds, 2021, 885: 160949.

[9] 卢秉恒，李涤尘. 增材制造(3D 打印)技术发展[J]. 机械制造与自动化，2013, 42(4): 1-4.
LU B H, LI D C. Development of the additive manufacturing (3D printing) technology[J]. Machine Building & Automation, 2013,

42(4): 1-4.

[10] 王华明. 高性能大型金属构件激光增材制造：若干材料基础问题[J]. 航空学报, 2014, 35(10): 2690-2698.
WANG H M. Materials' fundamental issues of laser additive manufacturing for high-performance large metallic components[J]. Acta Aeronautica et Astronautica Sinica, 2014, 35(10): 2690-2698.

[11] LOUVIS E, FOX P, SUTCLIFFE C J. Selective laser melting of aluminium components[J]. Journal of Materials Processing Technology, 2011, 211(2): 275-284.

[12] REDDY B V, DEEVI S C. Thermophysical properties of FeAl (Fe-40 at.% Al)[J]. Intermetallics, 2000, 8(12): 1369-1376.

[13] LI S, CAI B, DUAN R X, et al. Synchrotron characterisation of ultra-fine grain TiB_2/Al-Cu composite fabricated by laser powder bed fusion[J]. Acta Metallurgica Sinica (English Letters), 2021, 35 (1): 78-92.

[14] WANG J H, LIU T, LUO L S, et al. Selective laser melting of high-strength TiB_2/AlMgScZr composites: Microstructure, tensile deformation behavior, and mechanical properties [J]. Journal of Materials Research and Technology, 2022, 16: 786-800.

[15] PARSONS E M, SHAIK S Z. Additive manufacturing of aluminum metal matrix composites: Mechanical alloying of composite powders and single track consolidation with laser powder bed fusion [J]. Additive Manufacturing, 2022, 50: 102450.

[16] TREVISAN F, CALIGNANO F, LORUSSO M, et al. On the selective laser melting (SLM) of the AlSi10Mg alloy: Process, microstructure, and mechanical properties[J]. Materials, 2017, 10: 1-23.

[17] TANG M, PISTORIUS P C. Oxides, porosity and fatigue performance of AlSi10Mg parts produced by selective laser melting[J]. International Journal of Fatigue, 2017, 94: 192-201.

[18] ABOULKHAIR N T, EVERITT N M, ASHCROFT I, et al. Reducing porosity in AlSi10Mg parts processed by selective laser melting[J]. Additive Manufacturing, 2014, 1: 77-86.

[19] GARG P, JAMWAL A, KUMAR D, et al. Advance research progresses in aluminium matrix composites: Manufacturing & applications[J]. Journal of Materials Research and Technology, 2019, 8 (5): 4924-4939.

[20] MIRACLE D B. Metal matrix composites - from science to technological significance[J]. Composites Science and Technology, 2005, 65(15-16): 2526-2540.

[21] ESSIEN U A, VAUDREUIL S. In-situ metal matrix composites development for additive manufacturing: A perspective[J]. Journal of Achievements in Materials and Manufacturing Engineering, 2022, 111(2): 78-85.

[22] YU W H, SING S L, CHUA C K, et al. Particle-reinforced metal matrix nanocomposites fabricated by selective laser melting: A state of the art review[J]. Progress in Materials Science, 2019, 104: 330-379.

[23] WANG P, ECKERT J, PRASHANTH K G, et al. A review of particulate-reinforced aluminum matrix composites fabricated by selective laser melting[J]. Transactions of Nonferrous Metals Society of China, 2020, 30(8): 2001-2034.

[24] FENG Z, WANG X M, TAN H, et al. Effect of heat treatment patterns on porosity, microstructure, and mechanical properties of selective laser melted TiB_2/Al-Si-Mg composite [J]. Materials Science and Engineering: A, 2022, 855: 143932.

[25] BOILLAT R, ISANAKA S P, LIOU F. The effect of nanostructures in aluminum alloys processed using additive manufacturing on microstructural evolution and mechanical performance behavior [J]. Crystals, 2021, 11(5): 524.

[26] SHI J, WANG Y C. Development of metal matrix composites by laser-assisted additive manufacturing technologies: A review [J]. Journal of Materials Science, 2020, 55(23): 9883-9917.

[27] SADEGHI B, CAVALIERE P, PRUNCU C I, et al. Architectural design of advanced aluminum matrix composites: A review of recent developments[J]. Critical Reviews in Solid State and Materials Sciences, 2022: 1-71.

[28] ANOOP J, SUYAMBURAJAN V A, BABU P S, et al. Analysis and experimental investigation of A356 aluminium alloy hybrid composites reinforced with Gr-Fe_3O_4-B_4C nanoparticles synthesised by selective laser melting (SLM)[J]. Journal of Nanomaterials, 2022, 2022: 7510499.

[29] KUSOGLU I M, GÖKCE B, BARCIKOWSKI S. Use of (nano-)additives in laser powder bed fusion of Al powder feedstocks: Research directions within the last decade [J]. Procedia CIRP, 2020, 94: 11-16.

[30] TANG S Y, UMMETHALA R, SURYANARAYANA C, et al. Additive manufacturing of aluminum-based metal matrix composites -a review [J]. Advanced Engineering Materials, 2021, 23(7): 2100053.

[31] WANG Z, QU R T, SCUDINO S, et al. Hybrid nanostructured aluminum alloy with super-high strength[J]. NPG Asia Materials, 2015, 7: e229.

[32] AMIRKHANLOU S, JI S X. A review on high stiffness aluminum-based composites and bimetallics [J]. Critical Reviews in Solid State and Materials Sciences, 2019, 45(1): 1-21.

[33] KARABULUT Y, ÜNAL R. Additive manufacturing of ceramic particle-reinforced aluminum-based metal matrix composites: A review[J]. Journal of Materials Science, 2022, 57: 19212-19242.

[34] FEREIDUNI E, GHASEMI A, ELBESTAWI M. Selective laser melting of aluminum and titanium matrix composites: Recent progress and potential applications in the aerospace industry [J]. Aerospace, 2020, 7(6): 77.

[35] MINASYAN T, HUSSAINOVA I. Laser powder-bed fusion of ceramic particulate reinforced aluminum alloys: A review[J]. Materials, 2022, 15(7): 2467.

[36] CHEN B, XI X, TAN C W, et al. Recent progress in laser additive manufacturing of aluminum matrix composites [J]. Current Opinion in Chemical Engineering, 2020, 28: 28-35.

[37] XI L X, GU D D, GUO S, et al. Grain refinement in laser manufactured Al-based composites with TiB_2 ceramic [J]. Journal of Materials Research and Technology, 2020, 9(3): 2611-2622.

[38] PRAMOD S L, BAKSHI S R, MURTY B S. Aluminum-based cast in situ composites: A review[J]. Journal of Materials Engineering and Performance, 2015, 24(6): 2185-2207.

[39] SINGH N, BELOKAR R M, WALIA R S. A critical review on advanced reinforcements and base materials on hybrid metal matrix composites[J]. Silicon, 2020, 14(2): 335-358.

[40] ESAKKIRAJ E S, SURESH S, MOORTHI N S V, et al. Study of

mechanical behaviour of stir cast aluminium based composite reinforced with mechanically ball milled TiB_2 nano particles [J]. Advanced Materials Research, 2014, 984-985: 410-415.

[41] LIU X, LIU Y, HUANG D, et al. Tailoring in-situ TiB_2 particulates in aluminum matrix composites[J]. Materials Science and Engineering: A, 2017, 705: 55-61.

[42] SETHI D, KUMAR S, CHOUDHURY S, et al. Synthesis and characterization of AA7075/TiB_2 aluminum matrix composite formed through stir casting method[J]. Materials Today: Proceedings, 2020, 26: 1908-1913.

[43] 甘贵生,杨滨. TiB_2/7075 铝基复合材料流变挤压成形工艺[J]. 中国有色金属学报, 2014, 24(5): 1133-1140.
GAN G S, YANG B. Rheo-casting forming process of TiB_2/7075 aluminium matrix composites[J]. The Chinese Journal of Nonferrous Metals, 2014, 24(5): 1133-1140.

[44] GUO L P, WANG H Z, WEI Q L, et al. A comprehensive model to quantify the effects of additional nano-particles on the printability in laser powder bed fusion of aluminum alloy and composite[J]. Additive Manufacturing, 2022, 58: 103011.

[45] DING H, XIAO Y K, BIAN Z Y, et al. Effect of in-situ TiB_2 particles on microstructure and mechanical properties of Al-Fe-Ni manufactured by selective laser melting [J]. Materials Science and Engineering: A, 2022, 845: 143065.

[46] SUN T T, XIAO Y K, LUO G D, et al. Roadmap to improve the printability of a non-castable alloy for additive manufacturing[J]. Metallurgical and Materials Transactions A, 2022, 53: 2780-2795.

[47] LI X P, JI G, CHEN Z, et al. Selective laser melting of nano-TiB_2 decorated AlSi10Mg alloy with high fracture strength and ductility [J]. Acta Materialia, 2017, 129: 183-193.

[48] WANG Q Z, LIN X, KANG N, et al. Effect of laser additive manufacturing on the microstructure and mechanical properties of TiB_2 reinforced Al-Cu matrix composite[J]. Materials Science and Engineering: A, 2022, 840: 142950.

[49] WANG R Q, XI L X, DING K, et al. Powder preparation during ball milling and laser additive manufacturing of aluminum matrix nanocomposites: Powder properties, processability and mechanical property[J]. Advanced Powder Technology, 2022, 33(8): 103687.

[50] XIAO Y K, BIAN Z Y, WU Y, et al. Effect of nano-TiB_2 particles on the anisotropy in an AlSi10Mg alloy processed by selective laser melting[J]. Journal of Alloys and Compounds, 2019, 798: 644-655.

[51] XIAO Y K, CHEN H, BIAN Z Y, et al. Enhancing strength and ductility of AlSi10Mg fabricated by selective laser melting by TiB_2 nanoparticles[J]. Journal of Materials Science & Technology, 2022, 109: 254-266.

[52] XIAO Y K, YANG Q, BIAN Z Y, et al. Microstructure, heat treatment and mechanical properties of TiB_2/Al-7Si-Cu-Mg alloy fabricated by selective laser melting[J]. Materials Science and Engineering: A, 2021, 809: 140951.

[53] BIFFI C A, BASSANI P, FIOCCHI J, et al. Selective laser melting of AlCu-TiB_2 alloy using pulsed wave laser emission mode: Processability, microstructure and mechanical properties[J]. Materials & Design, 2021, 204: 109628.

[54] NIETO A, BISHT A, LAHIRI D, et al. Graphene reinforced metal and ceramic matrix composites: A review[J]. International Materials Reviews, 2016, 62(5): 241-302.

[55] HUANG X, YIN Z Y, WU S X, et al. Graphene-based materials: Synthesis, characterization, properties, and applications[J]. Small, 2011, 7(14): 1876-1902.

[56] EDWARDS R S, COLEMAN K S. Graphene synthesis: Relationship to applications[J]. Nanoscale, 2013, 5(1): 38-51.

[57] WITKIN D B, LAVERNIA E J. Synthesis and mechanical behavior of nanostructured materials via cryomilling[J]. Progress in Materials Science, 2006, 51(1): 1-60.

[58] SUTHAR J, PATEL K M. Processing issues, machining, and applications of aluminum metal matrix composites[J]. Materials and Manufacturing Processes, 2017, 33(5): 499-527.

[59] RAMANATHAN A, KRISHNAN P K, MURALIRAJA R. A review on the production of metal matrix composites through stir casting-furnace design, properties, challenges, and research opportunities[J]. Journal of Manufacturing Processes, 2019, 42: 213-245.

[60] DONG M Q, ZHOU W W, KAMATA K, et al. Microstructure and mechanical property of graphene oxide/AlSi10Mg composites fabricated by laser additive manufacturing[J]. Materials Characterization, 2020, 170: 110678.

[61] ZHOU W W, DONG M Q, ZHOU Z X, et al. In situ formation of uniformly dispersed Al_4C_3 nanorods during additive manufacturing of graphene oxide/Al mixed powders[J]. Carbon, 2019, 141: 67-75.

[62] TIWARI J K, MANDAL A, SATHISH N, et al. Investigation of porosity, microstructure and mechanical properties of additively manufactured graphene reinforced AlSi10Mg composite[J]. Additive Manufacturing, 2020, 33: 101095.

[63] ZHAO Z Y, BAI P K, MISRA R D K, et al. AlSi10Mg alloy nanocomposites reinforced with aluminum-coated graphene: Selective laser melting, interfacial microstructure and property analysis[J]. Journal of Alloys and Compounds, 2019, 792: 203-214.

[64] WANG Y C, SHI J, LU S Q, et al. Investigation of porosity and mechanical properties of graphene nanoplatelets-reinforced AlSi10Mg by selective laser melting[J]. Journal of Micro and Nano-Manufacturing, 2018, 6(1): 010902.

[65] WU L Y, ZHAO Z Y, BAI P K, et al. Wear resistance of graphene nano-platelets (GNPs) reinforced AlSi10Mg matrix composite prepared by SLM[J]. Applied Surface Science, 2020, 503: 144156.

[66] GUIDERDONI C, PAVLENKO E, TURQ V, et al. The preparation of carbon nanotube (CNT)/copper composites and the effect of the number of CNT walls on their hardness, friction and wear properties[J]. Carbon, 2013, 58: 185-197.

[67] SAVALANI M M, NG C C, LI Q H, et al. In situ formation of titanium carbide using titanium and carbon-nanotube powders by laser cladding[J]. Applied Surface Science, 2012, 258(7): 3173-3177.

[68] MASANTA M, SHARIFF S M, ROY CHOUDHURY A. Evaluation of modulus of elasticity, nano-hardness and fracture toughness of TiB_2-TiC-Al_2O_3 composite coating developed by SHS and laser cladding[J]. Materials Science and Engineering: A, 2011, 528 (16-17): 5327-5335.

[69] BASKARAN S, SELVAN B M M, ANANDAKRISHNAN V, et al. Effect of heat treatment on wear behavior of hot extruded

AA7075-4%TiC in situ metal matrix composite[J]. Applied Mechanics and Materials, 2014, 541-542: 263-267.

[70] PANDEY U, PUROHIT R, AGARWAL P, et al. Effect of TiC particles on the mechanical properties of aluminium alloy metal matrix composites (MMCs)[J]. Materials Today: Proceedings, 2017, 4(4): 5452-5460.

[71] SUI Y W, CHEN X, WANG R, et al. Wear behavior of in-situ TiC particles reinforced aluminum matrix composite [J]. Journal of Wuhan University of Technology-Mater. Sci. Ed., 2017, 32: 552-556.

[72] GENG R, QIU F, JIANG Q-C. Reinforcement in Al matrix composites: A review of strengthening behavior of nano-sized particles [J]. Advanced Engineering Materials, 2018, 20(9): 1701089.

[73] PANDEY U, PUROHIT R, AGARWAL P, et al. Study of fabrication, testing and characterization of Al/TiC metal matrix composites through different processing techniques [J]. Materials Today: Proceedings, 2018, 5(2): 4106-4117.

[74] AKINWAMIDE S O, ABE B T, AKINRIBIDE O J, et al. Characterization of microstructure, mechanical properties and corrosion response of aluminium-based composites fabricated via casting - a review [J]. The International Journal of Advanced Manufacturing Technology, 2020, 109(3-4): 975-991.

[75] FAN Z J, LI C, YANG H L, et al. Effects of TiC nanoparticle inoculation on the hot-tearing cracks and grain refinement of additively-manufactured AA2024 Al alloys [J]. Journal of Materials Research and Technology, 2022, 19: 194-207.

[76] 贾增庆, 高通, 王桂龙, 等. 激光选区熔化 2024 改性 AlSi10Mg 合金[J]. 中国有色金属学报, 2022, 32(11): 3257-3267.
JIA Z Q, GAO T, WANG G L, et al. Selective laser melting of 2024-modified AlSi10Mg alloy[J]. The Chinese Journal of Nonferrous Metals, 2022, 32(11): 3257-3267.

[77] WANG Y C, SHI J. Effect of hot isostatic pressing on nanoparticles reinforced AlSi10Mg produced by selective laser melting[J]. Materials Science and Engineering: A, 2020, 788: 139570.

[78] ZHOU Y, WEN S F, WANG C, et al. Effect of TiC content on the Al-15Si alloy processed by selective laser melting: Microstructure and mechanical properties[J]. Optics & Laser Technology, 2019, 120: 105719.

[79] GU D D, WANG H Q, DAI D H, et al. Densification behavior, microstructure evolution, and wear property of TiC nanoparticle reinforced AlSi10Mg bulk-form nanocomposites prepared by selective laser melting[J]. Journal of Laser Applications, 2015, 27: S17003.

[80] TAN Q Y, YIN Y, FAN Z Q, et al. Uncovering the roles of LaB_6-nanoparticle inoculant in the AlSi10Mg alloy fabricated via selective laser melting[J]. Materials Science and Engineering: A, 2021, 800: 140365.

[81] MAIR P, GOETTGENS V S, RAINER T, et al. Laser powder bed fusion of nano-CaB_6 decorated 2024 aluminum alloy[J]. Journal of Alloys and Compounds, 2021, 863: 158714.

[82] SHINKARYOV A S, OZHERELKOV D Y, PELEVIN I A, et al. Laser fusion of aluminum powder coated with diamond particles via selective laser melting: Powder preparation and synthesis description[J]. Coatings, 2021, 11(10): 1219.

[83] XUE G, KE L D, LIAO H L, et al. Effect of SiC particle size on densification behavior and mechanical properties of SiC_p/AlSi10Mg composites fabricated by laser powder bed fusion[J]. Journal of Alloys and Compounds, 2020, 845: 156260.

[84] XUE G, KE L D, ZHU H H, et al. Influence of processing parameters on selective laser melted SiC_p/AlSi10Mg composites: Densification, microstructure and mechanical properties[J]. Materials Science and Engineering: A, 2019, 764: 138155.

[85] WANG M, SONG B, WEI Q S, et al. Improved mechanical properties of AlSi7Mg/nano-SiC_p composites fabricated by selective laser melting[J]. Journal of Alloys and Compounds, 2019, 810: 151926.

[86] YI J C, ZHANG X W, RAO J H, et al. In-situ chemical reaction mechanism and non-equilibrium microstructural evolution of (TiB_2+TiC)/AlSi10Mg composites prepared by SLM-CS processing[J]. Journal of Alloys and Compounds, 2021, 857: 157553.

[87] CHANG F, Gu D D, DAI D H, et al. Selective laser melting of in-situ Al_4SiC_4+SiC hybrid reinforced Al matrix composites: Influence of starting SiC particle size[J]. Surface and Coatings Technology, 2015, 272: 15-24.

[88] DAI D H, GU D D, XIA M J, et al. Melt spreading behavior, microstructure evolution and wear resistance of selective laser melting additive manufactured AlN/AlSi10Mg nanocomposite[J]. Surface and Coatings Technology, 2018, 349: 279-288.

[89] DAI D H, GU D D, POPRAWE R, et al. Influence of additive multilayer feature on thermodynamics, stress and microstructure development during laser 3D printing of aluminum-based material[J]. Science Bulletin, 2017, 62(11): 779-787.

[90] LI X W, LI G, ZHANG M X, et al. Novel approach to additively manufacture high-strength Al alloys by laser powder bed fusion through addition of hybrid grain refiners [J]. Additive Manufacturing, 2021, 48: 102400.

[91] HE P D, LIU Q, KRUZIC J J, et al. Machine-learning assisted additive manufacturing of a TiCN reinforced AlSi10Mg composite with tailorable mechanical properties [J]. Materials Letters, 2022, 307: 131018.

[92] MIAO K, ZHOU H, GAO Y P, et al. Laser powder-bed-fusion of Si_3N_4 reinforced AlSi10Mg composites: Processing, mechanical properties and strengthening mechanisms[J]. Materials Science and Engineering: A, 2021, 825: 141874.

[93] KONOPATSKY A S, KVASHNIN D G, CORTHAY S, et al. Microstructure evolution during AlSi10Mg molten alloy/BN mi croflake interactions in metal matrix composites obtained through 3D printing[J]. Journal of Alloys and Compounds, 2021, 859: 157765.

[94] MARCHESE G, AVERSA A, LORUSSO M, et al. Development and characterisation of aluminium matrix nanocomposites AlSi10Mg/$MgAl_2O_4$ by laser powder bed fusion[J]. Metals, 2018, 8(3): 175.